RESEARCH ARTICLE

Aspergillus infection monitored by multimodal imaging in a rat model

Tomas Pluhacek[1,2], Milos Petrik[3], Dominika Luptakova[1,4], Oldrich Benada[1], Andrea Palyzova[1], Karel Lemr[1,2] and Vladimir Havlicek[1,2]

[1] Institute of Microbiology of the CAS, v.v.i., Prague, Czech Republic
[2] Regional Centre of Advanced Technologies and Materials, Department of Analytical Chemistry, Faculty of Science, Palacky University, Olomouc, Czech Republic
[3] Institute of Molecular and Translational Medicine, Faculty of Medicine and Dentistry, Palacky University, Olomouc, Czech Republic
[4] Department of Pharmacology, Jessenius Faculty of Medicine, Comenius University Bratislava, BioMed Martin, Slovakia

Although myriads of experimental approaches have been published in the field of fungal infection diagnostics, interestingly, in 21st century there is no satisfactory early noninvasive tool for *Aspergillus* diagnostics with good sensitivity and specificity. In this work, we for the first time described the fungal burden in rat lungs by multimodal imaging approach. The *Aspergillus* infection was monitored by positron emission tomography and light microscopy employing modified Grocott's methenamine silver staining and eosin counterstaining. Laser ablation inductively coupled plasma mass spectrometry imaging has revealed a dramatic iron increase in fungi-affected areas, which can be presumably attributed to microbial siderophores. Quantitative elemental data were inferred from matrix-matched standards prepared from rat lungs. The iron, silver, and gold MS images collected with variable laser foci revealed that particularly silver or gold can be used as excellent elements useful for sensitively tracking the *Aspergillus* infection. The limit of detection was determined for both ^{107}Ag and ^{197}Au as 0.03 μg/g (5 μm laser focus). The selective incorporation of ^{107}Ag and ^{197}Au into fungal cell bodies and low background noise from both elements were confirmed by energy dispersive X-ray scattering utilizing the submicron lateral resolving power of scanning electron microscopy. The low limits of detection and quantitation of both gold and silver make ICP-MS imaging monitoring a viable alternative to standard optical evaluation used in current clinical settings.

Received: November 29, 2015
Revised: March 20, 2016
Accepted: March 30, 2016

Keywords:
Animal model / Aspergillosis / Biomedicine / Fungal infection / Inductively coupled plasma / Mass spectrometry / Multimodal imaging

Additional supporting information may be found in the online version of this article at the publisher's web-site

1 Introduction

At present about one billion people worldwide are affected by fungal infections and these episodes are associated with 1.5 million deaths per annum [1]. Out of these cases, the invasive pulmonary aspergillosis accounts for more than 200 000 infections each year with an associated mortality rate

Correspondence: Dr. Vladimir Havlicek, Institute of Microbiology of the CAS, Videnska 1083, 142 20 Prague 4, Czech Republic
E-mail: vlhavlic@biomed.cas.cz

Abbreviations: **CT**, computed tomography; **GMS**, Grocott's methenamine silver; **ICP-MS**, inductively-coupled plasma mass spectrometry; **ITO**, indium-tin oxide; **LA**, laser ablation; **PET**, positron emission tomography; **pHPMA**, poly[N-(2-hydroxypropyl)methacrylamide] polymer; **SEM-EDS**, scanning electron microscopy-energy dispersive X-ray spectroscopy; **TAFC**, triacetylfusarinine C

Significance of the study

Aspergillus fumigatus, an airborne saprophytic fungus, can cause a variety of pulmonary syndromes including allergic bronchopulmonary aspergillosis, chronic pulmonary aspergillosis, and invasive pulmonary aspergillosis. In immunocompromised patients the invasive aspergillosis represents a life-threatening disease with a short survival time. Currently, there is a strong societal demand for the development and validation of new and sensitive molecular tools for early diagnosis of aspergillosis. Our work represents the first study ever that describes *Aspergillus* infection in a tissue by MS imaging. We present here a new sensitive approach for pathogen detection based on gold, silver, and iron imaging of fungal bodies in rat lungs by laser ablation ICP-MS. Low background and a wide dynamic range in Ag and Au quantitative determination together with lateral resolution getting close to the fungal hyphae diameter make our approach a viable alternative to standard but semiempiric optical microscopy and positron emission tomography that are also used in a multimodal approach in this study.

of 30–90% [2]. *Aspergillus* species represent the main cause of invasive fungal infections in patients with hematological malignancies and are a major cause of morbidity and mortality in immunocompromised patients in general [3]. The suspicion is high in patients with persistent febrile neutropenia and specific findings on CT (computed tomography), i.e. halo signs and air crescents [3, 4]. The classical mycological investigation (blood cultures, microscopy, serology) is frustrating due to the lack of sensitivity and/or specificity tests in this setting of patients [5]. With suspicious chest CT and negative serum galactomannan antigen detection, bronchoalveolar lavage can be requested. At the same time, detection of β-(1,3)-D-glucan, the application of a lateral flow device [6] and/or *Aspergillus* DNA by PCR can be useful, although some of these methods are not incorporated into European Organization for Research and Treatment of Cancer/Mycoses Study Group criteria due to a lack of standardization [7]. The main caveat of antigen detection-driven diagnosis of invasive pulmonary aspergillosis and other fungal infections in immunocompromised patients is a lack of positive prediction value.

In our quest for fungal biomarkers with high predictive value we focused on microbial siderophores [8]. Upon infected tissue examination we soon realized that the unequivocal localization of the diagnostic components is barely possible by using a single imaging technique. We thereby switched to a multimodal approach and probed molecular and elemental MS imaging [9–11], scanning electron microscopy-energy dispersive X-ray spectroscopy (SEM-EDS), positron emission tomography (PET), and CT for monitoring the fungal infection in a rat model [12].

2 Materials and methods

2.1 Chemicals and reagents

In standard animal models we used cyclophosphamide (Endoxan, Baxter, Czech Republic); teicoplanin (Targocid, Sanofi, Czech Republic); ciprofloxacin (Ciprofloxacin Kabi, Fresenius Kabi, Czech Republic); polymyxin E (Colomycin, Forest Laboratories, UK); ketamine (Calypsol, Gedeon Richter, Hungary); xylazine (Xylazin Ecuphar, Ecuphar, Germany); isoflurane (Forane, Abbvie, Czech Republic); and atropine (Atropin Biotika, Biotika, Czech Republic). The synthesis of ^{68}Ga-triacetylfusarinine C (TAFC) was described elsewhere [13].

In MS imaging experiments we applied nitric acid (65%, Analpure®), hydrogen peroxide (30%, PA+ grade), iron, silver, gold and INT-MIX element standards that were purchased from Analytika Ltd., Czech Republic. Milli-Q water (Millipore, France) had a resistivity of 18.2 MΩ/cm. High purity iron(III) chloride hexahydrate, gold chloride and silver nitrate were purchased from Sigma–Aldrich, Czech Republic, and indium-tin oxide glass slides (ITO) were obtained from Bruker Daltonics (Germany). In optical microscopy we used a silver stain kit containing periodic acid solution, gold chloride solution, sodium thiosulfate solution, silver methenamine, and borax solution (Sigma–Aldrich). Eosin-Y was obtained from VWR Chemicals, Czech Republic.

2.2 Pathogen cultivation and infection models

Aspergillus fumigatus 1059 CCF was obtained from the Culture Collection of Fungi, Faculty of Science, Charles University in Prague, and maintained on yeast medium slants (0.3% malt extract, 0.3% yeast extract, 0.5% peptone, 0.5% glucose) at 4°C. The inoculum was prepared from a culture performed on yeast medium plates at 30°C for 7 days until fully conidiated. Conidia were harvested by flooding the culture plate with PBS containing 0.1% Tween 80, and filtered through 1.0 μm nitrocellulose membrane filter (Whatman, UK) to remove hyphae. Spore concentration was counted in a hemacytometer.

All animal experiments were conducted in accordance with regulations and guidelines of the Czech Animal Protection Act (No. 246/1992), and with the approval of the Czech Ministry of Education, Youth and Sports (MSMT-21235/2013-12), and the institutional Animal Welfare Committee of the Faculty of Medicine and Dentistry of Palacky University in

Olomouc. The studies were performed using female Lewis rats (Anlab, Prague, Czech Republic).

The immunocompromised rats were intratracheally (left lobe) inoculated with 150 μL of *A. fumigatus* spores (10^7–10^8 colony forming units per mililiter). The infection was controlled by PET/CT imaging (Albira PET/SPECT/CT small animal imaging system; Bruker Biospin Corporation, Woodbridge, VA, USA) 1 h after a retro-orbital application of TAFC labeled with ^{68}Ga (4–6 MBq). A 10-min PET scan (axial FOV 148 mm) was performed, followed by a CT scan (axial FOV 65 mm, 45 kVp, 400 μA, at 600 projections). Scans were reconstructed with the Albira software using the likelihood expectation maximization and filtered back projection algorithms. After reconstruction, acquired data were viewed and analyzed with PMOD software (PMOD Technologies Ltd., Zurich, Switzerland). 3D images were obtained using VolView software (Kitware, Clifton Park, NY, USA). Rats were sacrificed by overdosing with ketamine/xylazine (2:1) after the imaging and lungs were removed for further investigations. Three sample sets were compared: the collapsed infected lungs, infected lungs inflated with poly[*N*-(2-hydroxypropyl)methacrylamide] polymer (pHPMA) [14], and control animals dosed just with immunosuppressants. The imaging data were collected on three biological replicates on the completed day 3 after inoculation.

2.3 Cryosectioning and histological staining

The deeply frozen native infected and control lung tissue samples were allowed to warm up to ca. −20°C prior to the sectioning with a Leica cryomicrotome CM1950 (Germany). The tissues were cut to 15 or 30 μm slices dedicated to SEM or laser ablation ICP-MS (LA-ICP-MS), respectively. The sections were thaw-mounted onto precooled ITO glass slides and vacuum-dried in desiccator at room temperature for 40 min. Adaptation of Grocott's methenamine silver (GMS) staining and eosin counterstaining was used for histology evaluation with light microscope Leica DM2000 (Germany). Note that prior to further use the pathogen was inactivated in glutaraldehyde vapors.

In the procedure, the mucopolysaccharide components of the fungal cell wall were oxidized by periodic acid to release aldehyde groups. The aldehyde groups then reacted with methenamine silver in the impregnation step, reducing it to metallic silver and rendering fungal cells visible. The addition of gold chloride was then used for toning and substitution of silver to gold by ion exchange. The fixation and eosin counterstaining, as well as some of the preceding steps could generate artifacts making the whole process semiempiric. Semiquantitative data are based on the number of black pixels divided by the total examined area [15] and can be determined by ImageJ software [16].

2.4 Scanning electron microscopy

The 15 μm rat lung cryosections on ITO glass surface were examined in an FEI Nova NanoSEM 450 high-resolution scanning electron microscope equipped with a CBS concentric backscatter detector for high-resolution imaging of nonconductive samples and an EDAX Octane Plus detector for EDS analysis and elemental mapping. The complete dried lung cryosection was visualized using Navigation Montage option of the SEM software (magnification 120x). The final image was then correlated with optical scan image of the same cryosection. This allowed us to precisely select the areas for high-resolution imaging in the SEM and subsequent EDS analysis.

2.5 Quantitative laser ablation ICP MS

An Analyte G2 LA system (Photon Machines, USA) equipped with an ArF excimer nanosecond laser (193 nm) was used for tissue ablation. Coupling of the LA and a 7700x ICP-MS (Agilent Technologies, Japan) was achieved with a Tygon® (1.2 m × 4 mm) tubing. An octopole reaction cell in helium mode allowed us to overcome spectral interferences observed on ^{56}Fe. The concentration and homogeneity of Fe in the digested matrix-matched standards was accessed separately by conventional solution ICP-MS with a MicroMist concentric nebulizer and a Scott-type double-pass spray chamber. The raw data were imported as .csv files to ImageLab multisensor imaging software [17] and distribution maps were correlated with the corresponding histological images.

The elemental quantitative data were inferred from LA-ICP-MS analysis of matrix-matched calibration standards analyzed in 1.5 mm line scans. The calibration points for iron and silver were recorded at 0, 60, 100, 150, 220 and 0, 0.1, 1, 10, 100, 1000 μg/g, respectively (Supporting Information Fig. 1). The background-subtracted signal intensity data were averaged over two line scans per concentration level and subsequently plotted against the concentrations obtained by ICP-MS after microwave-assisted acid digestion. The linear relationships were established with correlation coefficients ranging from 0.988 to 1.000 for all calibration curves.

2.6 Preparation of matrix-matched calibration standards

Frozen rat lungs were allowed to warm up to room temperature overnight. The lung tissues were rinsed multiple times in deionized water to remove residual blood and then homogenized using an ULTRA-TURRAX® T 18 basic variable speed tissue homogenizer (IKA®, Germany). The homogenate was stored overnight at 4°C and then the aliquots were spiked with iron standard yielding the requested concentration (Supporting Information Fig. 1). Each matrix-matched standard

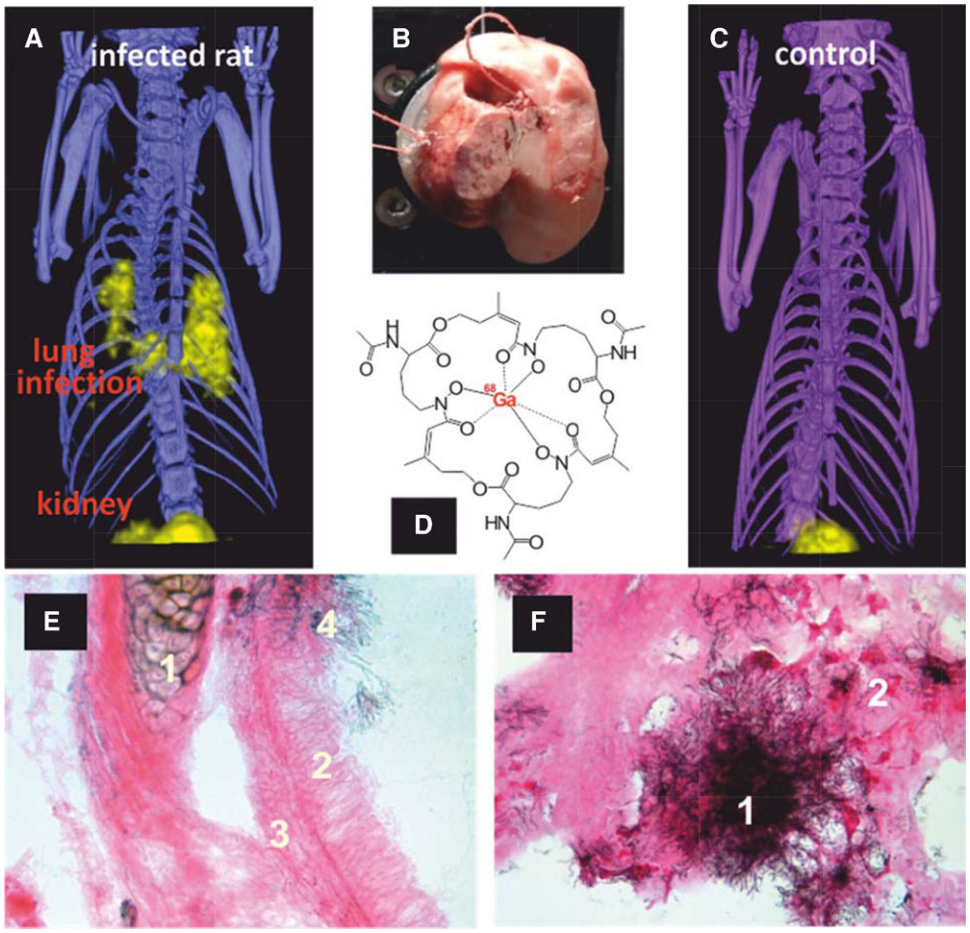

Figure 1. *Aspergillus* infection in rat lungs. (A and C) 3D volume rendered PET/CT images of infected and noninfected (control) animals in which the ferriform of TAFC was substituted by radioactive ^{68}Ga-TAFC (D). (B) Infected lung tissue in a cryomicrotome. (E) GMS-stained lung slice indicating the details of tracheal wall: (1) hyaline cartilage; (2) ciliated columnar epithelium; (3) connective tissue; (4) fungal hyphae. (F) *Aspergillus fumigatus* mycelium in black (1) and hemorrhage (2).

prepared in this way was subsequently homogenized at 5000 rpm for 5 min in a polycarbonate probe pretreated with an acid and stored in polypropylene vials at −80°C until the homogeneity assay and LA-ICP-MS analysis. After a 10-s homogenization, three aliquots of approximately 50 mg of each standard were weighed and digested in a Milestone 1200 closed vessel microwave digestion unit by using 2 mL of 65% HNO_3 and 1 mL of 30% H_2O_2. The matrix-matched standards were then either digested and/or cryo sectioned. The digested samples were analyzed by conventional solution ICP-MS with scandium and yttrium as internal standards. The remaining frozen standards were cryosectioned into 30 μm thin slices, thaw-mounted onto ITO glass slides, and vacuum-dried for LA-ICP-MS analysis. In addition, the quantitative LA-ICP-MS analysis of silver and gold was based on metal spiking of the rat lung homogenate, which was previously cryosectioned into 30 μm sections. After spiking with increasing concentrations of Ag and Au (0.2 μL of 0.1, 1, 10, 100, and 1000 μg/g) the calibration spots were allowed to dry at room temperature.

3 Results and discussion

3.1 Aspergillosis in rat lungs

In our setup, the immunocompromised animals did not survive 5 or 6 days of infection. The rats were therefore sacrificed on day 3, their lungs extracted, and filled with polymer or kept empty and intact (Fig. 1B). Silver (GMS-modified) eosin staining has revealed an extensive fungal burden in infected animals manifested by dense hyphae growth from cell wall of the lung tissue into aerial regions of bronchioles and alveoli (Fig. 1E and F). Optical microscopy provided morphological details including hyaline cartilage, ciliated columnar epithelium, and connective tissue as well as hemorrhage and lung

tissue damage. As there was a tendency for this stain to produce a lot of artefacts from background staining, the infection was also monitored by PET/CT.

In PET/CT experiment the animals were dosed with TAFC doped with gallium-68 isotope, which is a positron emitter (Fig. 1D). The ^{68}Ga-TAFC competes for ^{56}Fe-TAFC representing one of *A. fumigatus* siderophores [13]. These molecules and potential fungal virulence factors were then utilized for sensitive PET. The molecular sensitivity, defined as a combination of the probe and biological/physiological properties of the subject, can be as high as 10^{-11}–10^{-12} mol/L [18]. The infection was often localized in both lobes albeit to a different extent (Fig. 1A). Note the quite a limited spatial resolution in the low millimeter range. Positron signals were also abundant in kidneys, gastrointestinal tract, and urinary bladder (excretion route of ^{68}Ga-TAFC, details not shown). Although the lungs were carefully rinsed with water before being filled with polymer solution or kept intact, note an extensive hemorrhage in the tissue section (Fig. 1F).

3.2 Iron distribution in lungs

The biosynthesis of siderophores by pathogenic microorganisms to scavenge the iron from their hosts suggests these molecules as markers of fungal infection [8]. Our initial attempts to visualize siderophore ferri- or desferri-forms in tissues by MALDI-MS imaging failed due to either incompatibility of ionization with pHPMA polymer or limited dynamic range of the analysis. The lung tissue section contained too many air cavities and the actual tissue mass was low. We therefore switched to elemental MS imaging. The initial experiments indicated that the iron concentration in infected tissues was approx. 20 times higher compared to that in controls as accessed by quantitative LA-ICP-MS (Supporting Information Fig. 2). On the other hand, fungal infection was associated with extensive hemorrhage in the lungs (Fig. 1F) and the iron background coming from heme could potentially deteriorate the quantitative ferri-siderophore imaging MS data.

In reality, this interference was not as severe. The images obtained by ^{107}Ag LA-ICP-MS imaging truly followed the ^{56}Fe distribution data (Fig. 2) and both observed distributions corresponded well to light microscopy. More importantly, a better analytical dynamic range was achieved in silver quantitation in "macroscopic" view with 10 μm laser focus. The quantitation with matrix-matched standards prepared from rat lungs indicated much lower silver detection limit compared to that of iron (Supporting Information Fig. 1). LODs and LOQs were determined for silver and iron as 0.03, 0.10 and 0.7, 2.1 μg/g, respectively. Note that in ^{56}Fe quantitation we used higher laser focus and the octopole collision cell filled with helium to overcome ^{40}Ar^{16}O^{+} interference. The latter application was no longer needed for silver detection. It is also worth mentioning that iron was not detected in EDS analysis in either infected or control tissues (see below). On the contrary, the iron concentration in hyphae-containing regions was suspiciously high as revealed by LA-ICP-MS. As the iron is not coming from the staining procedure, we speculate that these elevated ^{56}Fe levels come from a diverse group of microbial siderophores. In our future work we will attempt to dereplicate those compounds using our recent tool Cyclobranch [19], which uses the isotopic data-filtering module and a siderophore database.

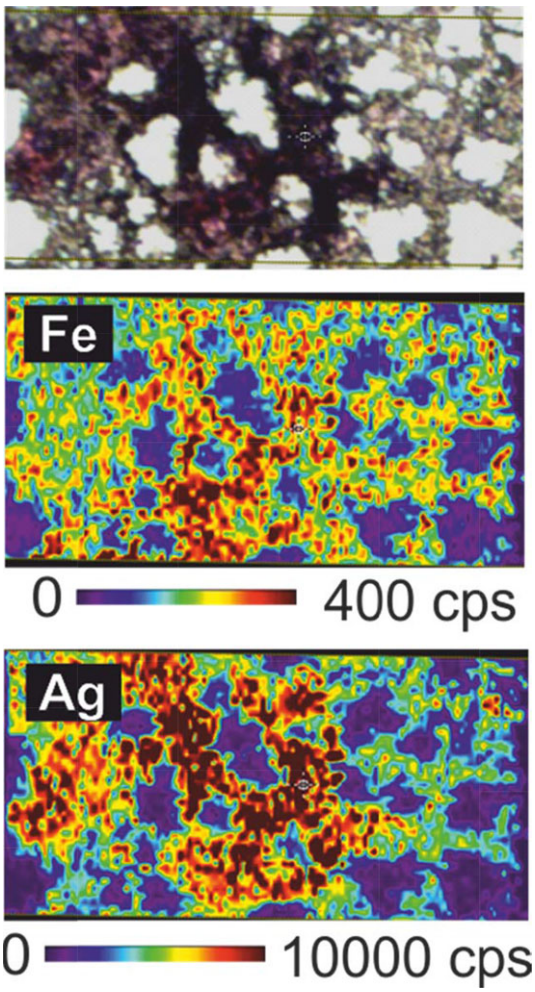

Figure 2. Optical image (top) and elemental distribution of ^{56}Fe (middle) and ^{107}Ag (bottom) in *Aspergillus*-infected lung tissue (filled with polymer). Repetition rate twenty hertz, laser energy density 1.06 J/cm^2, laser focus 10 μm, five shots per pixel, cps stands for detector response (count per second).

3.3 Gold and silver as specific and sensitive tracers of *Aspergillus* infection in tissue

The low silver detection limit in LA-ICP-MS enabled us to decrease the actual spot size to 3–5 microns, which is rather close to fungal hyphae ranging from 2 to 3 μm. Two separate dehydration protocols were tested on tissue sections, either

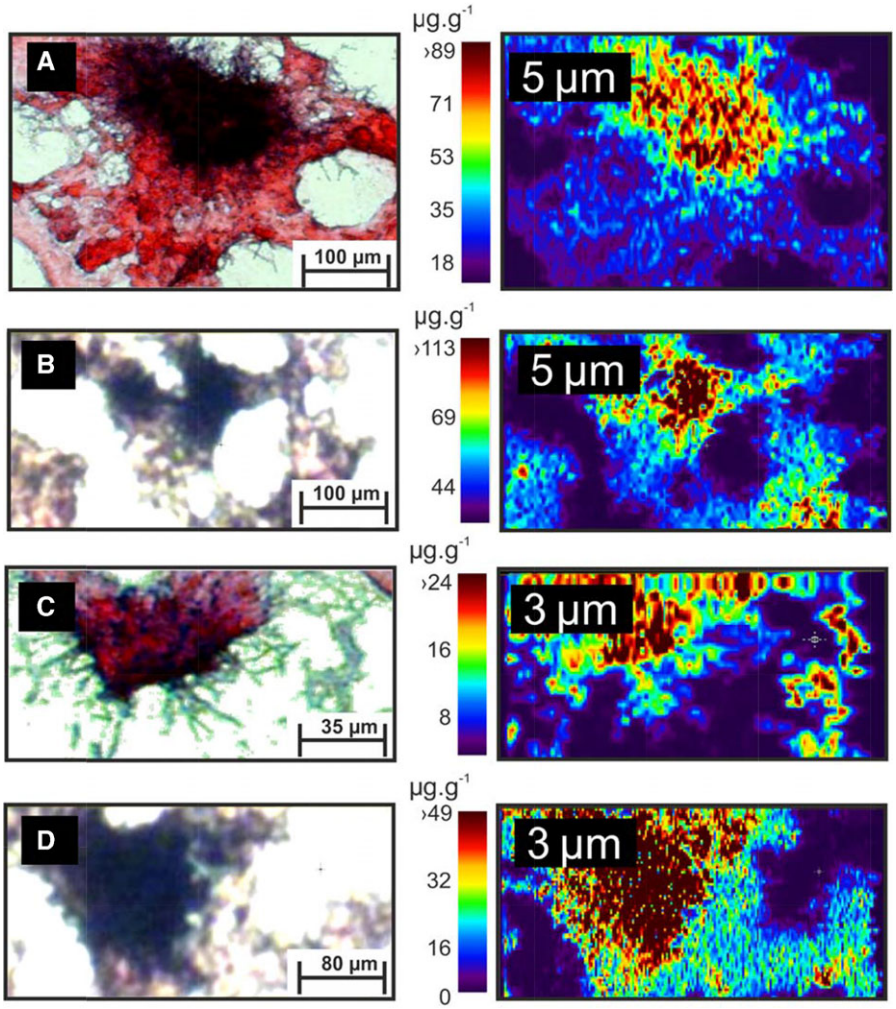

Figure 3. LA-ICP-MS ^{107}Ag distribution in infected tissue sections with 5 or 3 μm laser focus. (A and C) Dehydration made through graded ethanol series, (B and D) sections vacuum-dried in a desiccator.

through a graded ethanol series or vacuum-drying in desiccator (Fig. 3). The former technique was shown to be less sensitive, as a minor silver portion was removed by ethanol. Figure 3A showed no background silver signal in hemorrhage areas and even at 3 μm pixel size all the images were contrastive enough (Fig. 3C and D). ^{107}Ag was identified here as a more convenient element for infection tracking by LA-ICP-MS imaging than iron. The sufficient high dynamic range in silver detection might help microbiologists in aspergillosis diagnosis, namely in unclear decision cases (Fig. 2, bottom).

Similar or even better performance detection was achieved in gold monitoring by ICP-MS imaging. During the staining process, ^{197}Au was used for toning the histological image and was dosed at concentrations analogous to silver. LA-ICP-MS quantitative experiments have revealed the LOD and LOQ as 0.03 and 0.07 μg/g, respectively (Supporting Information Fig. 1). Mutual comparison of optical image with elemental distribution both of Ag and Au showed excellent consistency (Fig. 4). Monitoring these elements provides a high dynamic range and sensitivity at 5 micron lateral resolution.

Upon the laser ablation, most of the material was removed and ITO background glass surface was recovered. This observation triggered our attempt to estimate the actual material quantity desorbed from a single pixel. We weighed the fresh as well as dried 30 μm rat lung sections filled with polymer and calculated the slice area (Supporting Information Fig. 3). The calculations showed that the effectively desorbed element is in low femtogram range even for a wide 30 μm laser focus. This amount was sufficient for elemental imaging experiments but may not be enough for molecular MS imaging. From the quantitation point of view, the lung tissue containing either the polymer or a lot of air cavities represents a difficult material to work with.

Possible artefact formation was studied by SEM. SEM with its inherent extreme lateral resolution confirmed massive aspergillosis in infected animals and provided morphological details on hyphae spreading within the lung tissue (Fig. 5A). EDS analyses of background spots have indicated the presence of silicon, indium, and tin coming from ITO glass (Fig. 5B). Silver and gold peaks in EDS spectra collected

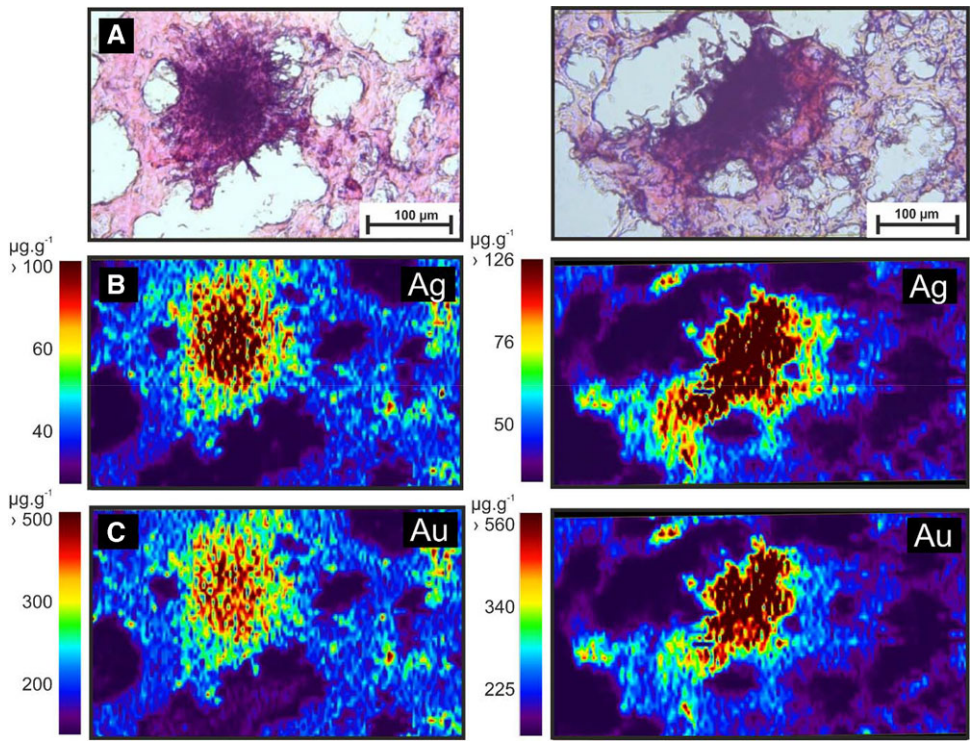

Figure 4. Optical image (A) and elemental distributions of ^{107}Ag (B) and ^{197}Au (C) in *Aspergillus*-infected lung. The LA-ICP-MS data were collected with 5 µm laser focus and dehydration of the sections was made either through graded ethanol series (all left) or in a desiccator (all right).

from *Aspergillus* hyphae revealed the specific accumulation of Ag and Au into fungal bodies during the GMS-eosin staining procedure (Fig. 5C). The selective accumulation of silver and gold in fungal bodies and negligible presence of both elements in the background was observed in many tested areas (Supporting Information Fig. 4). No iron was detected in any EDS analysis. Gold is thereby suggested as another prospective candidate suitable for monitoring the fungal infection upon silver (GMS-modified)-eosin treatment.

4 Concluding remarks

In this work we showed that a single imaging modality is not sufficient for getting the distribution of fungal biomarkers in lungs. In our specific case, molecular MS imaging of *Aspergillus*-specific siderophores failed, as the signals in MALDI-MS imaging of fungal siderophores in rat lung tissue sections were compromised by the inflating pHPMA as well as low analytical dynamic range. On the contrary, elemental MS imaging combined with GMS and eosin staining

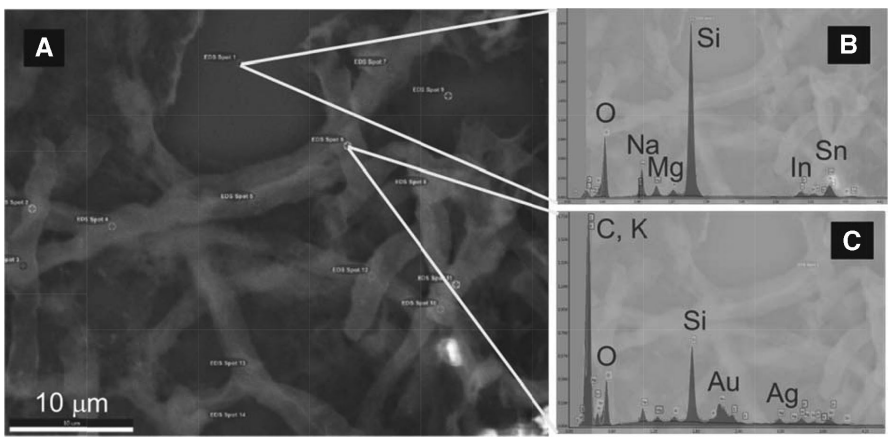

Figure 5. (A) SEM image with spot selection for elemental analysis in an infected tissue section (GMS-eosin staining, 15 kV, primary magnification 8000x), (B) EDS spectrum of a background-ITO glass surface spot, and (C) EDS spectrum of spot collected from *Aspergillus* hyphae.

provided reliable images of fungal hyphae deposition in tissues. The iron coming from siderophore ferriforms cannot be used as a proper disease tracer due to substantial iron background signal coming from erythrocytes flooding the inflamed bronchioles and alveoli. On the contrary, ^{107}Ag and ^{197}Au imaging provided by LA-ICP-MS exhibited sufficient sensitivity and low background noise. We demonstrated the images with 3–5 μm laser focus on silver- and gold-stained sections of infected lungs. Although EDS analysis has a limited dynamic range, the SEM images provided great morphology details in the submicrometer range confirming specific silver and gold incorporation into microbial hyphae. This approach has a substantial potential to become a more sensitive alternative to current standard visualization tools used in clinical mycology.

The manuscript was written through contributions of all the authors. A.P. was responsible for general microbiology, M.P. provided the PET/CT data, T.P. carried out the LA-ICP measurements and sectioning, D.L. performed the sectioning and histology, O.B. operated EM; K.L. and V.H. wrote the paper. The authors gratefully acknowledge the help of Lukas Krasny (IMIC) and Zbynek Novy (IMTM) in the early stages of manuscript preparation. The support from Ministry of Education, Youth, and Sports of the Czech Republic (LO1509, LO1304, LO1305), Czech Science Foundation (P206/12/1150), and by Operational Program Prague-Competitiveness project (CZ.2.16/3.1.00/24023) is also acknowledged.

The authors have declared no conflict of interest.

5 References

[1] Brown, G. D., Denning, D. W., Levitz, S. M., Tackling human fungal infections. *Science* 2012, *336*, 647.

[2] Thornton, C. R., Breaking the mould—novel diagnostic and therapeutic strategies for invasive pulmonary aspergillosis in the immune deficient patient. *Expert Rev. Clin. Immunol.* 2014, *10*, 771–780.

[3] Choi, S. H., Kang, E. S., Eo, H., Yoo, S. Y. et al., *Aspergillus* galactomannan antigen assay and invasive aspergillosis in pediatric cancer patients and hematopoietic stem cell transplant recipients. *Pediatr. Blood Cancer* 2013, *60*, 316–322.

[4] Faber, E., Riegrova, D., Jarosova, M., Hubacek, J. et al., Abdominal zygomycotic: thromboangiitis in a patient with AML and t(1;13;14). *Ann. Hematol.* 1996, *73*, 195–198.

[5] Havlicek, V., Lemr, K., Schug, K. A., Current trends in microbial diagnostics based on mass spectrometry. *Anal. Chem.* 2013, *85*, 790–797.

[6] Eigl, S., Prattes, J., Lackner, M., Willinger, B. et al., Multicenter evaluation of a lateral-flow device test for diagnosing invasive pulmonary aspergillosis in ICU patients. *Crit. Care* 2015, *19*, 178.

[7] White, P. L., Parr, C., Thornton, C., Barnes, R. A., Evaluation of real-time PCR, galactomannan enzyme-linked immunosorbent assay (ELISA), and a novel lateral-flow device for diagnosis of invasive aspergillosis. *J. Clin. Microbiol.* 2013, *51*, 1510–1516.

[8] Pluháček, T., Lemr, K., Ghosh, D., Milde, D. et al., Characterization of microbial siderophores by mass spectrometry. *Mass Spectrom. Rev.* 2016, *35*, 35–47.

[9] Sussulini, A., Becker, J. S., Application of laser microdissection ICP-MS for high resolution elemental mapping in mouse brain tissue: a comparative study with laser ablation ICP-MS. *Talanta* 2015, *132*, 579–582.

[10] Boehme, S., Staerk, H.-J., Kuehnel, D., Reemtsma, T., Exploring LA-ICP-MS as a quantitative imaging technique to study nanoparticle uptake in *Daphnia magna* and zebrafish (*Danio rerio*) embryos. *Anal. Bioanal. Chem.* 2015, *407*, 5477–5485.

[11] Drescher, D., Giesen, C., Traub, H., Panne, U. et al., Quantitative imaging of gold and silver nanoparticles in single eukaryotic cells by laser ablation ICP-MS. *Anal. Chem.* 2012, *84*, 9684–9688.

[12] Haas, H., Petrik, M., Decristoforo, C., An iron-mimicking, trojan horse-entering fungi—has the time come for molecular imaging of fungal infections? *PLoS Pathog.* 2015, *11*, e1004568.

[13] Petrik, M., Haas, H., Laverman, P., Schrettl, M. et al., Ga-68-triacetylfusarinine C and Ga-68-ferrioxamine E for *Aspergillus* infection imaging: uptake specificity in various microorganisms. *Mol. Imaging Biol.* 2014, *16*, 102–108.

[14] Strohalm, M., Strohalm, J., Kaftan, F., Krasny, L. et al., Poly N-(2-hydroxypropyl)methacrylamide-based tissue-embedding medium compatible with MALDI mass spectrometry imaging experiments. *Anal. Chem.* 2011, *83*, 5458–5462.

[15] O'Dea, E. M., Amarsaikhan, N., Li, H. T., Downey, J. et al., Eosinophils are recruited in response to chitin exposure and enhance Th2-mediated immune pathology in *Aspergillus fumigatus* infection. *Infect. Immun.* 2014, *82*, 3199–3205.

[16] Schindelin, J., Rueden, C. T., Hiner, M. C., Eliceiri, K. W., The ImageJ ecosystem: an open platform for biomedical image analysis. *Mol. Reprod. Dev.* 2015, *82*, 518–529.

[17] Ofner, J., Kamilli, K. A., Eitenberger, E., Friedbacher, G. et al., Chemometric analysis of multisensor hyperspectral images of precipitated atmospheric particulate matter. *Anal. Chem.* 2015, *87*, 9413–9420.

[18] Levin, C. S., New imaging technologies to enhance the molecular sensitivity of positron emission tomography. *Proc. IEEE* 2008, *96*, 439–467.

[19] Novak, J., Lemr, K., Schug, K. A., Havlicek, V., CycloBranch: de novo sequencing of nonribosomal peptides from accurate product ion mass spectra. *J. Am. Soc. Mass Spectrom.* 2015, *26*, 1780–1786.

